EWOD-CONTROLLED DUAL LIQUID PRISM FOR ADAPTIVE BEAM STEERING

Jiangtao Cheng*
*Author for correspondence
Department of Mechanical Engineering
Virginia Tech
Blacksburg, VA 24061, USA
E-mail: chengjt@vt.edu

H. Felix Wu, Ph.D.
Office of Energy Efficiency & Renewable Energy
U.S. Department of Energy
1000 Independence Ave., SW
Washington, DC 20585
USA

ABSTRACT

Solar energy accounts for the greatest source of renewable energy on the earth. The use of photovoltaic (PV) and concentrating photovoltaic (CPV) technology has been the most promising method of harvesting solar energy. These CPV systems often require bulky motor-driven tracking devices to steer the sun's beams onto solar cells. The cost of providing and maintaining these tracking systems is the primary inhibitor for widespread application. The purpose of this work is to overcome the need for mechanical solar trackers through the use of an electrowetting-driven solar tracking (EWST) system. The electrowetting-driven solar tracking system consists of an array of novel electrowetting-assisted dual liquid prisms, which are filled with immiscible fluids that have large differences in refractive indices. The naturally formed meniscus between the fluids can function as a dynamic optical prism. Via the full-range modulation of the liquid prisms, incident sunlight can be adaptively tracked, steered, and focused onto concentrated photovoltaic cells through a fixed optical condenser (Fresnel lens). Furthermore, unlike the conventional, cumbersome motor-driven tracking systems used today, the liquid prism system introduced in this work would be suitable for rooftop application. The results of this work reveal that the EWST system has the potential to generate ~70% more green energy at 50% of the conventional PV capital cost.

NOMENCLATURE

θ	contact angle
ε	dielectric permittivity
γ	surface tension
d	dielectric thickness
θ_y	contact angle with no voltage applied
c	unit area capacitance of the dielectric
R	reflectance
n	refractive index

INTRODUCTION

Solar radiation is the largest source of renewable energy on earth; however, harvesting this wealth of energy on a commercial scale has proved difficult, owing to the fact that conventional methods of transforming solar radiation into electricity are highly inefficient. Conventionally, solar energy is harvested through the use of solar panels with photovoltaic (PV) or concentrating photovoltaic (CPV) solar cells (Luque and Andreev, 2007; Neufeld et al., 2008). However, these PV and CPV cells have run into the same problem: solar cells generate the most energy when the incident solar radiation is hitting the cell at a perpendicular angle. Once the incident radiation begins to hit the cells at an oblique angle, the efficiency drops sharply (Roth et al., 2004). Consequently, people began to devise various methods to track the sun throughout the day. By using methods such as mechanical trackers, people have been able to nearly double the energy output and increase efficiency by nearly 40% compared to stationary PV or CPV cells (Huang et al., 2011).

Today, the most common method of harvesting solar energy is through the use of concentrating photovoltaic (CPV) systems. Current CPV cells are significantly more efficient than traditional silicon-based photovoltaic cells (~40% compared to ~20%). However, the widespread use of these CPV cells has been slowed drastically due to the high cost of the multi-junction III-V cells. To reduce this cost, people have been developing optical condensers to focus solar radiation onto a smaller CPV cell to harvest the concentrated radiation. The vast majority of concentrators require a system to adaptively track the sun as it moves across the sky, therefore ensuring maximum energy harvesting throughout the entire day.

One of the most widely used solar tracking methods is through the use of mechanical, motor-driven dual-axis tracking systems. The use of mechanical trackers incurs additional complexity due to the increase in mechanical moving parts. In particular, bulky passive heat sinks or active cooling blankets are needed in order to ensure the CPV cells do not overheat and breakdown (Mousazadeh et al., 2009). The addition of all of these mechanical parts makes this type of system cost ineffective since it is very power-hungry. In addition, there is a staggering cost to maintain these systems. Lastly, the large, bulky and heavy mechanical system is not suitable for rooftop application.

To avoid the use of mechanical moving parts, Pender (2005) patented his motion-free tracking system, which is made up of a beam deflector and a fixed optical condenser that centers the radiation onto a small area. The beam deflectors are made of a pair of adjustable prism arrays made of liquid crystals. By applying varying degrees of intensity and distribution of an electric field, he was able to modulate the refractive index of the liquid crystal. By changing the refractive index of the liquid crystal, the system is able to keep the direction of the deflected beam fixed while the incident beam shifts. Currie et al. (2008) put forward a different approach to harvesting solar radiation. Currie developed organic solar concentrators that are planar waveguides with light absorbed by a thin-film organic coating on a substrate surface. This system gives rise to a near 10-fold increase of power output due to the

near-field energy transfer of solid-state solvation. The only problem with this technique is the fact that these organic coatings are only stable for 3 months, making it unsuitable for a long-term energy solution. Furthermore, long-term maintenance would be costly since organic coatings generally need a strong adhesive to bind to the substrate.

Another approach demonstrated by Kotsidas et al. (2011) is the use of nominally stationary high-concentration solar concentrators based on gradient-index lenses. These gradient lenses would enable daylong flux concentration on a large order. However, due to the high fabrication cost of these lenses, it faces the same problem of CPV cells, in that it is very difficult to progress up to a commercial scale. Baker et al. (2012) introduced an optical system that is able to self-track the sun. The system uses voltage-induced refractive index modulation of nanoparticle dispersion to achieve self-tracking capabilities. In their initial experiments they found that in order to change the local index it would take substantial energy inputs. It is evident that further optimization is needed in order to achieve the required index response to make the system cost-effective.

This paper introduces an electrowetting-on-dielectric (EWOD) mechanism that controls a single and a novel dual liquid prism with an aperture size of ≥ 10mm x 10mm. The system is driven by a custom-built control unit that can be programmed to adaptively track incident radiation onto a desired location with a high degree of agility. As a result, the liquid prism can work as an electrowetting solar module for adaptive solar tracking. This EWOD system will be able to track the sun without bulky mechanical moving parts. The key points for this system are that it has very low energy consumption, quiet operation, and low profile, making it suitable for rooftop applications.

BACKGROUND

In this paper we have designed and fabricated an EWOD-controlled single liquid prism module and a novel EWOD-driven dual liquid prism module for adaptive solar tracking and sunlight steering. The electrowetting on dielectric effect controls the contact angle between an electrolyte and a dielectric surface through the use of an electric field (Lee et al., 2002; Mugele and Baret, 2005; Jones, 2005). Originally a liquid droplet rests atop a solid substrate with a contact angle θ_y (Fig. 1). When a voltage is applied to the embedded electrode, the contact angle θ_y is changed to θ due to the electro-hydrodynamic effect. A mathematical relationship between the wettability change θ and contact angle θ_y and the applied voltage is given by the Young-Lippmann equation (Vallet et al., 1996):

$$cos\theta = cos\theta_y + \frac{\varepsilon V^2}{2d\gamma_{wo}} \qquad (1)$$

where ε is the dielectric permittivity, γ is the surface tension between two fluids (in this case water and oil), d is the dielectric thickness, and θ_y is the water contact angle with no voltage applied.

Although EWOD is a relatively new technique, there have already been some applications and significant advancements within this field. These applications include chip-level spot cooling (Cheng and Chen, 2010a,b), adjustable liquid lens (Kuiper and Hendriks, 2004; Murade et al., 2011), clinical diagnostics (Srinivasan et al., 2004), and electronic paper (Hayes and Feenstra, 2003). There have been some reported studies that created micro liquid prisms for beam steering as well (Smith et al., 2006; Hou et al., 2007). However, the aperture sizes of the liquid prisms in these studies were relatively small (from a few hundred microns to <5mm). Due to the small aperture sizes, widespread application has been highly constrained. Moreover, the dual prism design demonstrated in this paper has never been experimentally presented either.

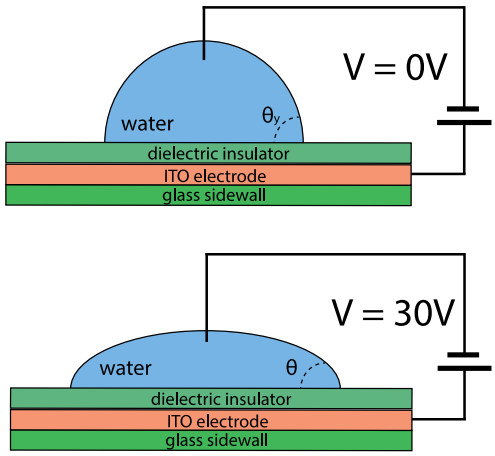

Fig.1. Electrowetting phenomenon schematic.

MATERIALS & METHODS

We have designed and fabricated an electrowetting-based single liquid prism module for adaptive solar tracking and steering (shown in Fig. 2). The geometry of the single prism module was designed to be 10mm x 10mm x 20mm. We diced indium tin oxide (ITO) glass substrates ($R_{\square}$ ~ 20Ω) into four pieces of 10mm x 20mm each using a glass saw (MTI Corporation, MT-4 4-inch Trim Saw); these slides will work as the module's sidewalls. The sidewalls were then cleaned with a glass detergent, Alconox (Sigma-Aldrich, 242985), and were subsequently ultra-sonicated in a bath of acetone for three minutes. We then attached four copper wires via silver epoxy (MG Chemicals 8331-14G) to the top of each sidewall. The silver epoxy was allowed to cure at 65ºC for 25 minutes. These copper wires will be used for voltage control signal input. Then we applied UV epoxy (Norland Electronic Adhesive 123) to assemble the four sidewalls into an open square channel. Afterwards we conformally coated ~1-µm-thick parylene C onto the ITO sidewalls. Parylene C is the material used for the dielectric barrier. Next we dip-coated the glass channels in fluoropolymer (Cytonix, PFC 1601V), which was then baked at 120ºC for 12 hours. To dip-coat, we carefully dipped the channel into the fluoropolymer for five seconds, then removed

the channel and rested it on a cotton paper for five seconds to allow the extra fluoropolymer to be pulled away. The sidewalls are coated with fluoropolymer to make them hydrophobic and therefore reducing the driving voltage to operate the module and the whole system. Applying this thin fluoropolymer film across the sidewalls also ensures the channel surface is free of defections, such as the formation of pinholes, which would otherwise allow the applied voltage to hydrolyze the water held within the module. Then we diced a 30mm x 30mm indium tin oxide substrate to act as the base of the module. This base substrate was cleaned following the same procedure stated above. We attached another copper wire onto the edge of the base substrate using silver epoxy. This wire will be used to ground the module and the entire system. Finally, we attached the glass channel onto the base substrate using UV epoxy to form a liquid prism module shown in Figure 2.

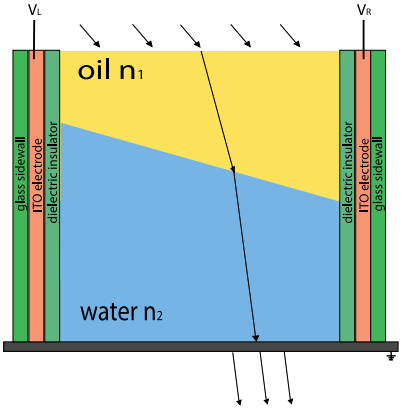

Fig. 2. A cross sectional view of the single prism redirecting incident sunlight.

We filled the module with two immiscible fluids, e.g., DI water and silicone oil. We dissolved 1% wt. sodium dodecyl sulfate (Sigma Aldrich 71725-50G) and 0.01% Potassium Chloride (Sigma Aldrich P9333-500G) into the water. The dissolved sodium dodecyl sulfate (SDS) into the water can adjust and lower the equilibrium surface tension between water and silicone oil. Potassium Chloride was dissolved into the water to improve its electrical conductivity. The density of this solution was then experimentally measured to be ~0.99714 g/mL. The silicone oil we used was Silicone Oil AR 20 (Sigma Aldrich 10835-100mL), which has a density of 1.01 g/mL. We chose fluids with near identical densities in order to avoid gravity-induced deformations, such as the Rayleigh-Taylor instabilities. Also, the silicone oil is very transparent; therefore, allowing the most amount of solar radiation to pass through. It is noteworthy that the silicone oil has very stable physical and chemical properties at extreme temperatures as well as a high refractive index (RI) contrast with water (Water, RI = 1.33; silicone oil AR 20, RI = 1.44). Importantly, the Snell's Law indicates that the higher the RI is, the lower the apex angle needs to be in order to achieve the same wide tracking range. We filled the modules with water first then the silicone oil. Figure 3 shows an image of the single prism at equilibrium with a natural curvature formed between water and silicone oil.

Fig. 3. Electrowetting-controlled single prism module at equilibrium with no voltage applied.

After some experimentation we improved this original design by incorporating dual prisms instead of a single prism. The dual prism module design would greatly increase the amount of energy harvested since it would have a far greater tracking range than a single prism module, thereby allowing more solar radiation to be directed to CPV cells. Figure 4 shows a schematic of the dual prism module. The fabrication of the dual prism module is exactly the same as the above stated procedures up until after the sidewalls are coated with the fluoropolymer. For the dual prism design, after coating the channel with fluoropolymer, two 1mm x 1mm double-sided adhesive copper tapes were attached to the east and west side walls of the glass channel. The tape is used because it is hydrophilic and will allow the water to adhere to or touch the sidewalls throughout the liquid prism modulation, which is necessary for the control voltage on the ITO electrodes to be effective. We also made some modifications on the 30mm x 30mm base substrate. In the single prism design, the electrolyte (water) is always in contact with the bare base ITO substrate. Due to this arrangement, the entire base substrate acts as the ground since the substrate is also an ITO electrode. However, in the dual prism design, the water will be suspended between two layers of oils, losing contact to the base substrate. In order to ground the electrolyte, we used a 6 mm long bare copper wire, which will be subsequently attached to the base substrate and then grounded. We made the wire 6 mm long since the wire needs to be in contact with the electrolyte during operation. We prepared the 6 mm long copper wire by cleaning it using acetone first. Following, we dip coated the wire in fluoropolymer. We dried the fluoropolymer at 95ºC for one hour. We coated the wire with fluoropolymer as the passivation layer in order to mitigate electrolyzation effects the wire may cause in the water. Also making the copper wire hydrophobic can avoid unfavorable influences such as the pinning of water on the wire. We then attached the 6-mm-long copper wire perpendicularly in the middle of the base substrate using silver epoxy. Subsequently we attached the open channel previously prepared to the base substrate using UV epoxy.

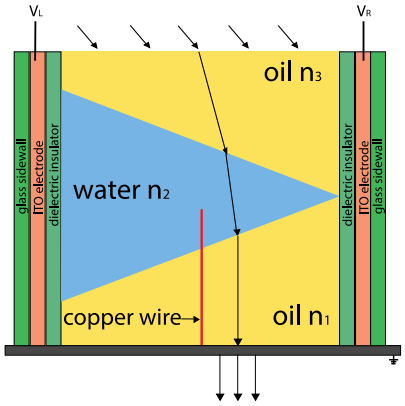

Fig. 4. A cross sectional view of the dual prism module redirecting incident sunlight.

We filled the module with three immiscible fluids in the sequence as shown in Fig. 5. We used the same water solution as prepared above and silicone oil AR 20. However, this time we added another silicone oil (Sigma Aldrich 378321-250mL) with a density of 0.93 g/mL and the refractive index of 1.403. We filled the modules in order of density, i.e., silicone oil AR 20 first, then the water solution, and finally the lighter silicone oil. When the fluids were inserted, the water formed an ellipse in between the two oils (as shown in Fig. 5). This phenomenon is due to the fact the side walls are ultra-hydrophobic with two 1mm x 1mm hydrophilic areas on opposite walls. The 1mm x 1mm hydrophilic areas attract the water thereby forming the characteristic ellipse illustrated in Fig. 5.

RESULTS AND DISCUSSION

Upon applying an alternating current (AC) voltage using the custom-built control unit to the east and west sidewalls, the oil-water interfaces can be adjusted in the module. We chose to use an alternating current voltage instead of a direct current (DC) voltage since long term application of DC voltage would permanently polarize the dielectric film, rendering it useless for future use. We adopted the frequency of AC voltage as low as possible since we aim to minimize the energy consumption of this entire system. We found that a frequency as low as 10 Hz could still keep the oil-water interface straight without any apparent fluid interface oscillation.

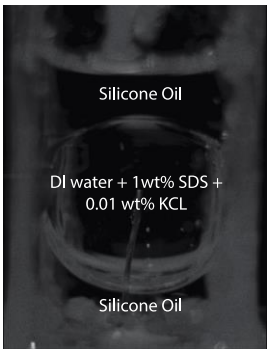

Fig. 5. Electrowetting-controlled dual prism module at equilibrium.

The balance of interfacial surface tensions at the water (*w*), oil (*o*) and fluoropolymer sidewall (*f*) contact zone is governed by this set of equations (Mugele and Baret, 2005):

$$\gamma_{wf} = \gamma_{fo} - \gamma_{wo}\cos\theta_y$$
$$\gamma_{wf}(V) = \gamma_{fo}(0) - \frac{1}{2}cV^2 \quad (2)$$

where c is the unit area capacitance of the dielectric, γ is the surface tension between two immiscible fluids, V the applied voltage, and θ_y the water contact angle with no voltage being applied. Equation 2 determines the voltages applied on the sidewalls in order to form a smooth fluid-fluid interface. Figure 6 displays some snapshots of the single prism under the indicated applied voltages.

Liquid prism orientation shown in image 6b would be activated during early morning when the sunlight is at a very slanted angle; in comparison, the interface orientation shown in image 6c would be triggered and maintained during late afternoon when the sun is also at a very oblique angle. Throughout the day, the liquid prism would gradually shift from image 6b to image 6c, tracking and redirecting the sun's beams accordingly as the sun moves across the sky.

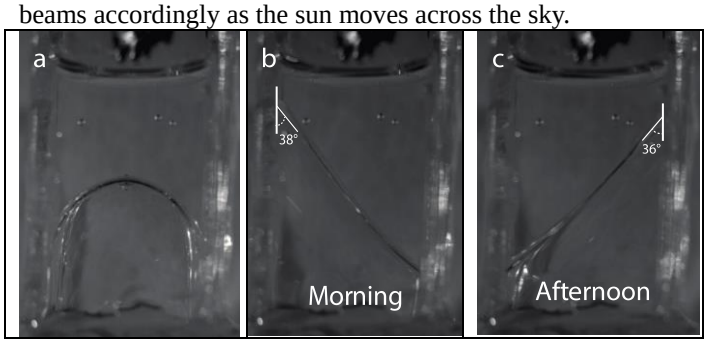

Fig. 6. Snapshots of an electrowetting-driven single liquid prism module. (a) Before applying voltage, a natural curved-shaped interface is formed. (b) The left sidewall is applied with 44V and the right sidewall with 10V. (c) When 44V is applied to the right sidewall and 10V applied to the left sidewall, the interface is reversely controlled. All voltages were applied at 10Hz.

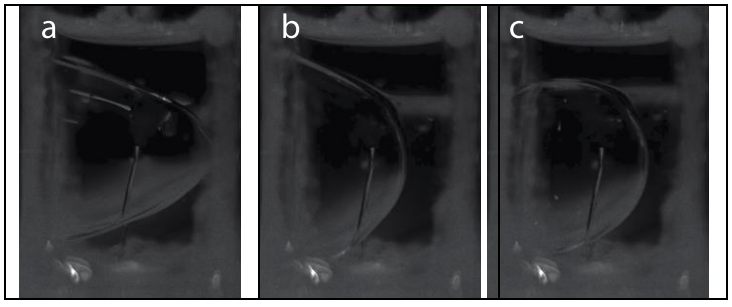

Fig. 7. Photographs of an electrowetting-driven dual liquid prism module without copper tape attached to opposite sidewalls. a) The left sidewall is applied with 34V and the right sidewall with 2V. b) Both the right and left sidewalls with 15V. c) 34V is applied to the right sidewall and 2V applied to the left sidewall. All voltages were applied at 10 Hz.

Further experimentation was conducted using the novel dual prism design. All of the previous parameters were used, except for the voltage applied. At first we tested if the dual prism could work without the copper tape attached to the east and west sidewalls. Figure 7 shows the dual prism without copper tape on the sidewalls under the indicated applied voltage.

We found that the water suspended within the oil would detach from the opposite sidewall, making it impossible for the water to be influenced by the applied voltage on the opposite sidewall. It is apparent that the double-sided adhesive copper tape is critical for this module design to function. We fabricated a new dual prism module following the procedure stated above. Figure 8 illustrates some snapshots of the dual prism under the documented applied voltages.

Figure 8 displays the range of modulation the dual prism is capable of. The interface orientation as shown in image 8a would be modulated during early morning, image 8b would be maintained during noon, while image 8c would be prompted during late afternoon. This module would be able to track the sun throughout the day by gradually shifting from image 8a to image 8c. The dual prism design is far more advantageous to the single prism design because it is able to direct incident sunlight over a greater range. This allows this system to harvest more solar radiation than the single prism system.

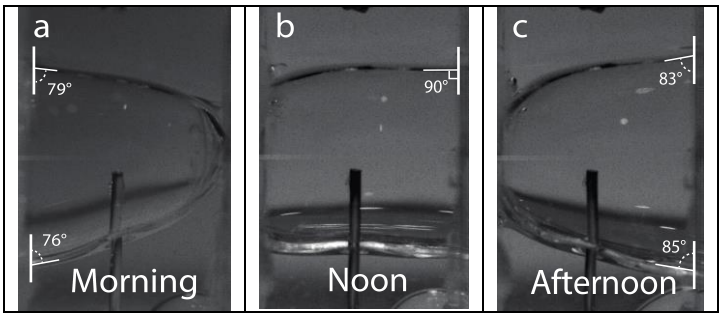

Fig. 8. Snapshots of an electrowetting-driven dual liquid prism module. a) The left sidewall is applied with 39V and the right sidewall with 2V. b) Both the right and left sidewalls with 15V. c) When 39V is applied to the right sidewall and 2V applied to the left sidewall, the interface is reversely controlled. All voltages were applied at 10Hz.

ANALYSIS

Optical analysis was carried out on both the single and dual prism modules. In both models there are three key components that need to be taken into consideration while calculating the theoretical efficiency: reflective loss due to the geometry of the module, loss of intensity of the incident radiation due to absorption, and reflective loss due to the interface made by the oil and water. The reflective loss due to the geometry of the module can be disregarded since an additional coating of an anti-reflective (AR) material would render this loss to be negligible. However, if a coating of an AR material cannot be applied, the reflective loss is proportional to the amount of beams between rays 1 and 2 as shown in Figure 9. All of the beams between rays 2 and 3 will be deflected through the prism. This statement holds true for both the single and dual prism.

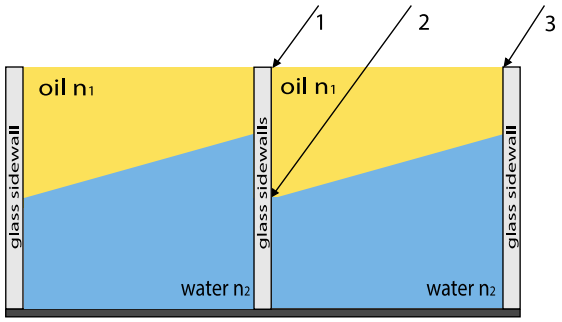

Fig. 9. Reflective loss due to the geometry of the module.

The next factor to account is the energy loss due to absorption in the fluids. The light intensity I decreases following this relationship: $I(x) = I_0 \exp[-4\pi kx/k_0]$, where I_0 is the original optical intensity, k_0 is the optical wavelength in vacuum, k is the absorption index of the medium and x the distance traveled (Cheng et al., 2013). This loss is negligible since the total distance the light has to travel through the fluids is very small (~ 4-6 cm). This small distance will only cause an estimated absorption loss of less than roughly 5% (Cheng et al., 2013).

Finally, the last and most significant reflective loss is due to the reflection on the oil and water interface. The two most important factors to consider is the amount of light being transmitted and the amount of light being reflected. From the laws of energy conservation, we know that the summation of the fraction of energy transmitted and the fraction of energy reflected should equal 1. Since electromagnetic waves are transverse, the calculation of the reflectance (R) depends on the polarization of the ray in the directions perpendicular to and parallel to the incident plane (Hecht, 2002):

$$R_s = \left|\frac{n_i \cos\theta_i - n_t \cos\theta_t}{n_i \cos\theta_i + n_t \cos\theta_t}\right|^2$$
$$R_p = \left|\frac{n_i \cos\theta_t - n_t \cos\theta_t}{n_i \cos\theta_t + n_t \cos\theta_t}\right|^2 \quad (3)$$

where R_s and R_p denote the reflectance of s and p polarized rays. However, since ambient solar radiation is not polarized, the reflectance is equal to the average of R_s and R_p (Cheng et al., 2013).

It is noteworthy that the dual prism design has a far greater tracking range than the single prism. Since there are two interfaces in the dual prism, incident beams have the capability of being refracted twice therein. With a greater tracking angle, the dual prism can refract extremely oblique angles of incident sunlight at early morning and late afternoon that a single prism design could not. With this in mind, we calculated the efficiency of the dual prism model using equations 3 and the Snell's Law and summarized the results in Table 1.

Table 1. Theoretical loss due to reflection for the dual prism module. n_1 and n_2 denote refractive indices.

n_1	n_2	Incident Angle	Reflection Loss (%)
1.33	1.44	45°	~25
		25°	~7
		0°	~7
1.33	1.403	45°	~27
		25°	~8
		0°	~7

The liquid prisms would be incorporated into an array fashion, which would redirect incident rays through a Fresnel lens underneath for further concentration. To redirect the rays through a Fresnel lens the exiting radiation from each liquid prism would have a normal incidence with respect to the lens. Figure 10 shows the setup for the optofluidic solar concentrators composed of liquid prism panel.

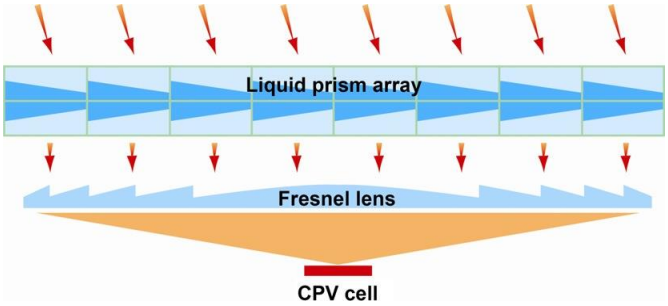

Fig. 10. Arrayed prism arrangement for significant solar beam steering (Cheng et al., 2013).

A theoretical cost analysis was also conducted to compare against conventional methods of solar harvesting. We used public information from Solfocus Inc. as well as Suntech Power for statistics on CPV tracking systems and PV systems, respectively. Table 2 summarizes the cost analysis findings. The results reveal that the EWST system has the potential to generate ~70% more green energy at 50% of the conventional PV capital cost.

Table 2. Theoretical cost analysis of the proposed dual system.

Parameter	PV System	CPV System	CPV w/dual prism
Efficiency	~17%	~40%	~20% - 37%
Area Size (for 100W)	5.3ft^2	2.25ft^2	3.16ft^2
Manufacturing Cost	$240	~$300	~$100
Rooftop Application	Yes	No	Yes

CONCLUSION

Solar photovoltaics, a technology that enables the direct conversion of solar radiation into usable electricity, is a promising alternative to help alleviate the energy crisis. However, the widespread implementation of this technology is not commercially feasible due to the high cost and relatively low efficiency of these state-of-the-art systems. In this paper we reported a novel optofluidic solar concentration design. The dual prism design has never been experimentally tested prior to this study. We have discussed in this paper a dual prism system design can (a) continually control the oil-water interface orientation with low power consumption, (b) agilely steer beams through the fluid–fluid interface, and (c) adaptively track the beam source (sun) without any mechanical moving parts. We conducted a theoretical efficiency and cost analysis on the proposed system. An array of the proposed dual prism design coupled with the utilization of small area ultra-high efficiency photovoltaic cells puts this system in close competition with conventional, cheaper alternatives such as coal or natural gas. Furthermore, the compact configuration of the module and panel makes this system a prime candidate for residential deployment, specifically on the rooftop.

Further work should consist of experimentally verifying the theoretical yields calculated in the paper. Moreover, as stated throughout the paper, one of the main objectives of this system is for rooftop application. Since all of our experiments were conducted on a flat surface, further experimentation is needed in determining how the slant of a rooftop will affect the agility and responsiveness of the system. We believe that if successfully implemented, this transformational optofluidic technology can make solar photovoltaic electric power generation systems not only economically competitive but also environmentally sustainable.

ACKNOWLEDGMENTS

This work was supported by China National Science Foundation (grant No. 51328601).

REFERENCES

[1] Antonio L. Luque and Viacheslav M. Andreev. 2007. Concentrator photovoltaics. Springer Series in Optical Sciences.

[2] Baker, K.A., Karp, J.H., Tremblay, E.J., Hallas, J.M., Ford, J.E., 2012. Reactive self-tracking solar concentrators: concept, design, and initial materials characterization. Applied Optics 51 (8), 1086–1094.

[3] Cheng, J.-T., Chen, C.-L., 2010a. Adaptive chip cooling using electrowetting on coplanar control electrodes. Nanoscale and Microscale Thermophysical Engineering 14 (2), 63–74.

[4] Cheng, J.-T., Chen, C.-L., 2010b. Active thermal management of on-chip hot spots using EWOD-driven droplet microfluidics. Experiments in Fluids 49 (6), 1349–1357.

[5] Cheng, J. -T., Cheng, C.-L., Park, S., 2013. Optofluidic solar concentrators using electrowetting tracking: Concept, design, and characterization. Solar Energy 89 .152–161

[6] Currie, M.J., Mapel, J.K., Heidel, T.D., Goffri, S., Baldo, M.A., 2008. High-efficiency organic solar concentrators for

photovoltaics. Science 321 (5886), 226–228. (3), 2325–2334.

[7] Hayes, R.A., Feenstra, B.J., 2003. Video-speed electronic paper based on electrowetting. Nature (London) 425, 383–385.

[8] E. Hecht, 2002. Optics 4

[9] Hou, L., Smith, N.R., Heikenfeld, J., 2007. Electrowetting manipulation of any optical film. Applied Physics Letters 90, 251114.

[10] Huang, B.J., Ding, W.L., Huang, Y.C., 2011. Long-term field test of solar PV power generation using one-axis 3-position sun tracker. Solar Energy 85 (9), 1935–1944.

[11] Jones, T.B., 2005. An electromechanical interpretation of electrowetting. Journal of Micromechanical and Microengineering 15, 1184–1187.

[12] Kotsidas, P., Modi, V., Gordon, J.M., 2011. Nominally stationary high concentration solar optics by gradient-index lenses. Optics Express 19

[13] Kuiper, S., Hendriks, B.H.W., 2004. Variable-focus liquid lens for miniature cameras. Applied Physics Letters 85 (7), 1128–1130.

[14] Lee, J., Moon, H., Fowler, J., Schoellhammer, T., Kim, C.J., 2002. Electrowetting and electrowetting-on-dielectric for microscale liquid handling. Sensors and Actuators A – Physical 95, 259–268.

[15] Mousazadeh, H., Keyhani, A., Javadi, A., Mobli, H., Abrinia, K., Sharifi, A., 2009. A review of principle and sun-tracking methods for maximizing solar systems output. Renewable and Sustainable Energy Reviews 13 (8), 1800–1818.

[16] Mugele, F., Baret, J.-C., 2005. Electrowetting: from basics to applications. Journal of Physics: Condensed Matter 17, R705–R774.

[17] Murade, C.U., Oh, J.M., van den Ende, D., Mugele, F., 2011. Electrow- etting driven optical switch and tunable aperture. Optics Express 19 (16), 15525–15531.

[18] Neufeld, C.J., Toledo, N.G., Cruz, S.C., Iza, M., DenBaars, S.P., Mishra, U.K., 2008. High quantum efficiency InGaN/GaN solar cells with 2.95 eV band gap. Applied Physics Letters 93 (14), 143502.

[19] Pender, J.G. 2005. Motion-free tracking solar concentrator. US patent No: 6958868 B1.

[20] Roth, P., Georgiev, A., Boudinov, H., 2004. Design and construction of a system for sun-tracking. Renewable Energy 29 (3), 393–402.

[21] Smith, N.R., Abeysinghe, D.C., Haus, J.W., Heikenfeld, J., 2006. Agile wide-angle beam steering with electrowetting microprisms. Optics Express 14 (14), 6557–6563.

[22] Srinivasan, V., Pamula, V.K., Fair, R.B., 2004. An integrated digital microfluidic lab-on-a-chip for clinical diagnostics on human physio- logical fluids. Lab on a Chip 4, 310–315.

[23] Vallet, M., Berge, B., Vovelle, L., 1996. Electrowetting of water and aqueous solutions on poly(ethylene terephthalate) insulating films. Polymer 37, 2465-2470.